Indian Journal of Fibre & Textile Research
Vol. 46, December 2021, pp. 354-360

Acoustical and thermal properties of different insulation layers for glass fibre/epoxy composites

Ersin Sayar[1], Nuray Ucar[2 a], Neslihan Karaca[3], Aysen Onen[3], Murat Baydogan[4], Erdem Selver[5], Cafer Kırbaş[6], Berkay Geygel[7] & Mehmet Ucar[7]

[1]Mechanical Engineering Department, [2]Textile Engineering Department, [3] Department of Chemistry , [4]Material Science and Engineering, Istanbul Technical University, Istanbul, Turkey

[5]Textile Engineering Department, Kahramanmaraş Sutcuimam University, Kahramanmaraş, Turkey

[6]Tubitak Ulusal Metrology Enstitusu, Gebze, Kocaeli, Turkey
[7]Automotive Engineering, Kocaeli University, Kocaeli, Turkey

Received 1 February 2021; revised received and accepted 27 July 2021

In the present study, novel insulation materials, such as nonwoven blankets with nanofibre webs, along with the conventional materials, such as stone wool blankets and nonwoven blankets containing silica aerogel for glass fibre fabric/epoxy composites, have been investigated experimentally. The results reveal that the nonwoven blankets containing nanofibres may replace the conventional stone wool insulation layers or nonwovens with silica aerogel insulation layer especially in the vibrational working conditions due to the brittle nature of both of these conventional materials.

Keywords: Acoustic properties, Glass fibre /epoxy composite, Nonwoven, Polyacrylonitrile nanofibre, Silica aerogel, Stone wool, Thermal insulation

1 Introduction

Glass fibres are commonly used in various applications due to their superior strength [1,2], light weight [3, 4], low cost [5, 6], good thermal properties [6-8], and acoustic properties [7-11]. They can be used in the forms of short fibres [12, 13], filament fibres [14, 15], or nonwovens[16, 17] to achieve the desired properties of fibre-reinforced composites. The acoustic and thermal properties of composite materials can be enhanced by adding/combining nano- and macroscale additives to glass fibres. Silica aerogels are reported as suitable additives to glass fibres[18-29].

Various studies have addressed the effect of aerogel on thermal conductivity and sound absorption in glass fibres[30-32]. Shafi *et al.* [33] investigated the improvement in thermal properties of silica aerogel glass fibre composites using the two-step sol-gel method. Haq *et al.* [34] investigated the thermal behaviour of silica aerogel glass fibre composites with silica sols ranging between 4% and 32%. Zhu *et al.* [35] manufactured glass fibre/polyimide aerogel composites (GF/PI) by impregnating glass fibres with 0%, 25%, 75%, and 100% mole of the rigid diamine, PPDA (*p*-phenylenediamine) as aerogels. Li *et al.* [36] studied the effect of H_2O:TEOS molar ratio of silica aerogels on mechanical, thermal, and flammability properties of glass fibre film/silica aerogel composites. Zhou *et al.* [37] measured mechanical properties and thermal stability of glass fibre reinforced silica aerogel composites.

Yang *et al.* [38] investigated the sound absorption performance of aerogel/ polyester-polyethylene nonwovens fabrics. Talebi *et al.* [39] investigated sound absorption properties of silica aerogel/polyester blankets, which were prepared by the sol-gel process. Forest *et al.* [40] compared the acoustic properties of silica aerogel granules with different sizes (80 μm and 3.5 mm) and glass wool samples. They observed that aerogels showed at least 10 dB higher acoustic transmission losses than glass wool with the same thickness.

In addition to aerogels, there has been growing interest in using polyacrylonitrile (PAN) fibres for their good thermal and sound absorption properties [41, 42]. Xiang *et al.* [43] investigated acoustic properties of polyacrylonitrile (PAN) nanofibrous membranes. Kucukali Ozturk *et al.* [44] investigated sound absorption performance, air permeability, and surface morphology of polyacrylonitrile nanofibre–coated nonwoven jute and wool structures. Their findings showed that coating

[a] Corresponding author.
E-mail: ucarnu@itu.edu.tr

of jute and wool felts with PAN decreased air permeability while improving sound absorption performance. Liu *et al.* [45] compared the sound absorptivity of polyacrylonitrile (PAN), thermoplastic polyurethane (TPU), and thermoplastic polyester elastomer (TPEE) nanofibres. They found that PAN fibres have higher sound absorption coefficients than TPU and TPEE when the frequency is 100–2500 Hz. Rabbi *et al.* [46]incorporated PAN nanofibre webs into the needle-punched PET and wool nonwoven layers. The results showed that sound transmission loss was improved by increasing the number of nanofibre layers, and higher transmission loss values were obtained. Sabetzadeh *et al*. [47] analyzed the effect of nanofibre diameter and web surface density on the thermal conductivity of polyacrylonitrile nanofibre webs. They observed that using thinner fibres with a higher surface density led to better thermal performance.

Stone wools are other effective materials used as thermal or sound insulators [48, 49]. Nagy *et al.* [50] investigated the thermal conductivity of stone wool structures for walkable roofs. They observed that the density and moisture content of the mineral wool affected the thermal conductivity. Andres *et al*. [51] compared the thermal properties of stone wool layered sandwich composites after exposing the composites to different levels of heating. Forouharmajd *et al.* [52] compared the acoustic performance of stone wool with plastics (at different densities and thicknesses). They observed that stone wool samples had higher absorption coefficient values than rubber samples.

The production of glass fibre/epoxy composites with silica aerogel should be carried out very carefully to avoid any kind of damage or degradation in mechanical properties. Agglomeration of silica aerogel particles can degrade the mechanical properties, leading to difficulties in the production of composites with both good thermal and mechanical properties. Thus, insulation of glass fibre/epoxy composite is generally carried out by using a blanket as insulation layer, such as stone wool. Nanofibre webs recently are implemented for sound insulation. However, they have not been explored for their use as an insulation layer together with glass fibre/epoxy composite, neither for sound nor for thermal insulation in industrial applications. Most of the studies in the literature have been carried out for thermal or acoustic properties only. Both thermal and acoustic properties are important at the same time for many application areas, such as insulation of vehicles (airplanes, etc.). Comparative studies between the different insulation materials are important for the final decision. In this study, a polypropylene nonwoven blanket with silica aerogel and same nonwoven blanket with PAN nanofibre web have been prepared for glass fibre/epoxy composites for improved properties without creating a negative effect on mechanical properties of glass/epoxy. Both thermal and acoustic properties of layers including commercial, conventional stone wool blanket and nonwoven with silica aerogel and nonwoven with PAN nanofibre web have been experimentally examined and compared for glass fibre/epoxy composite for the first time. Nonwoven blankets with PAN nanofibres or silica aerogels are produced using electrospinning process. Their sound and thermal properties are compared using impedance tubes and heat transfer coefficient test chamber respectively.

2 Materials and Methods

2.1 Materials

Plain woven glass fabric (525 g/m^2 areal density, 2 weft/cm, 2 warp/cm, and 0.4 mm thickness), epoxy resin (F-1564), and hardener (F-3486), purchased from Fibermak, were used. Commercially available silica aerogel ENOVA®MT 1200 (Cabot´s Aerogel), spunbond polypropylene nonwoven fabric, polyacrylonitrile, and stone wool were obtained from different local companies.

2.2 Production Methods

Nonwoven Blanket with PAN Nanofibre

Polyacrylonitrile (PAN) nanofibre web with 312 nm diameter [Fig. 1(a)] was produced by electrospinning system, which consists of a syringe pump, high voltage power supply, nozzle (needle 21 gauge), and electrically conductive collector. The working principle of electrospinning [Fig. 1(b)] includes feeding of PAN through syringe pump. PAN was first dissolved in dimethylformamide (DMF), and then placed into the nozzle that is connected to the syringe pump. The high voltage power supply is connected to the nozzle to charge polymer solution, which allows movement of solution jet from the tip of the nozzle into the electrically conductive collector (grounded). As the polymer solution jet moves from the tip of the nozzle to the surface of the collector, solvent is vaporized and polymer in nanofibre web structure is collected onto the surface of the collector [Figs 1(a) and (b)]. In this study, PAN was solved in 8wt% dimethylformamide (DMF). The electrospinning system has been set up with 14 kV voltage. The distance between the nozzle and the connector is kept 14 cm. In addition, 0.9 mL/h feeding rate and a 21-gauge needle (inner diameter 0.514 mm and outer diameter 0.819 mm) have been chosen as nozzle parameters. Nanofibre web was electrospun on polypropylene nonwoven layer which was placed on the collector. The thickness of the PAN nanofibre web and each nonwoven layer was approximately 0.085 mm.

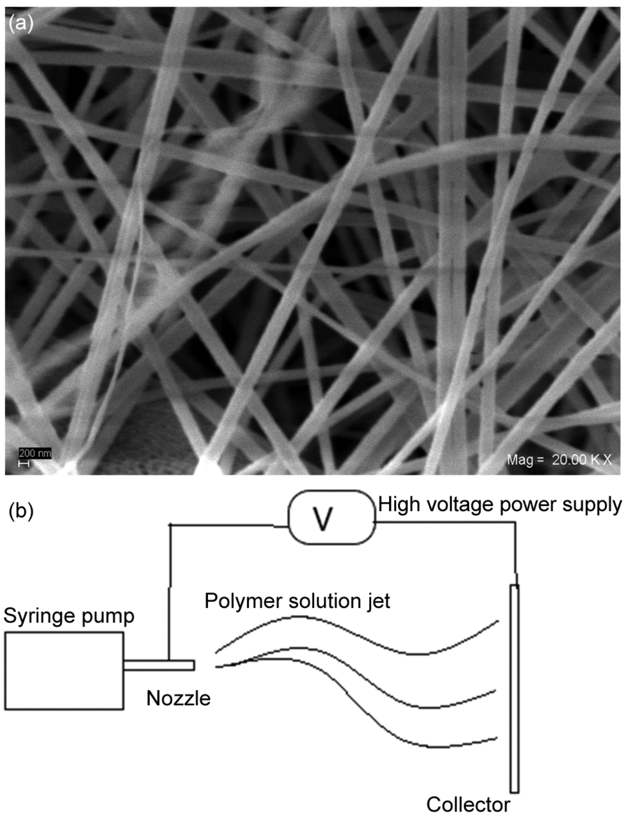

Fig. 1 — Images of (a) PAN nanofibre web with 312 nm diameter and (b) schematic illustration of electrospinning system

Nonwoven Blanket with Silica Aerogel Particle

Silica aerogel particle [Fig. 2(a)] was sprayed into nonwoven layers using the same electrospinning system. Silica aerogel particles were dispersed in DMF (SiO_2: DMF= 0.025 g : 1 mL) by ultrasonic homogenizer (Bandelin) for 3 h. Then, dispersed silica aerogel was sprayed into a polypropylene nonwoven layer [Fig. 2(b)], which was placed on an aluminium collector of the electrospinning system with 1 mL/h feeding rate, 16 kV voltage, and 15 cm distance between tip of the nozzle (21-gauge needle) and collector.

Glass Fibre/Epoxy Composite with Insulation Blankets

Glass fibre/epoxy composite (glass fibre volume fraction 62%) was produced by hand lay-up technique with 0/0 stacking sequence of 6 layers of glass woven fabric. The composite samples were cured in laboratory conditions for 2 days. After the curing process, all insulation blanket materials (stone wool blanket, nonwoven blanket with silica aerogel, and nonwoven blanket with PAN nanofibre web) were layered on glass fibre/epoxy composite [Table 1 and Figs 3(a) and (b)]. The insulation materials were placed right next to glass/epoxy composite, as shown in Fig. 3(c). The thickness of glass fibre/epoxy composite was kept about 3 mm, while the thicknesses of the insulation layers were in the range of 2 -2.5 mm. Thus, all composite materials with different insulation layers retain similar thicknesses (in the range of 5.0 - 5.5 cm) to compare their effect on the insulation performance.

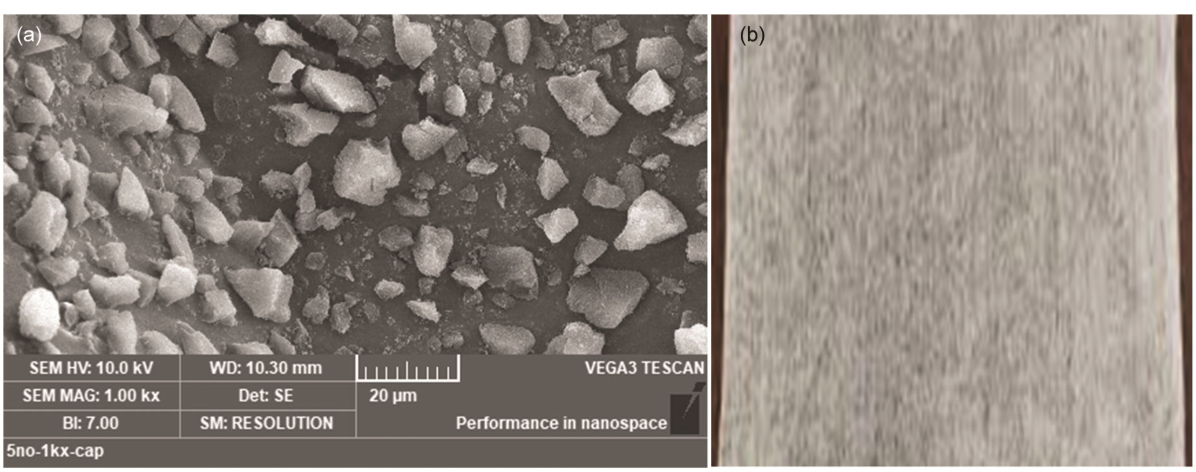

Fig. 2 — Images of (a) silica aerogel particle, and (b) nonwoven layer

Table 1 — Materials and sample properties

Code	Layers type	Stacking sequence	Thickness, mm	Areal density g/m^2
GCSA	Glass fibre/epoxy composite (6 layers)+ PP nonwoven (21 layers) and PP nonwoven with silica aerogel (4 layers)	4 layers nonwoven with aerogels 21 layers nonwoven 6 layers glass fabric composite	5.5	4965
GCPN	Glass fibre/epoxy composite (6 layers)+ PP nonwoven (17 layers) and PP nonwoven with PAN layer (4 PP nonwoven layer +4 PAN layers)	8 layers nonwoven with PAN (4 nonwoven+4 PAN) 17 layers nonwoven 6 layers glass fabric composite	5.5	4999
GCSW	Glass fibre/epoxy composite 96 layers)+ stone wool fibre blanket layer	Stone wool blanket 6 layers glass fabric composite	5.0	5068

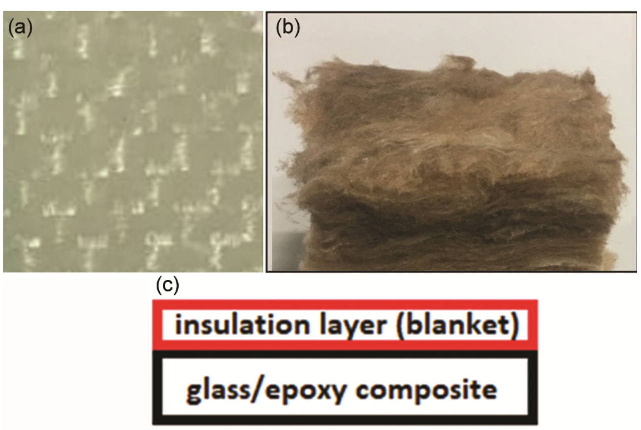

Fig. 3 — Images of (a) glass fibre/epoxy composite, (b) stone wool, and (c) schematic illustration of glass fibre/epoxy composite with insulation layers

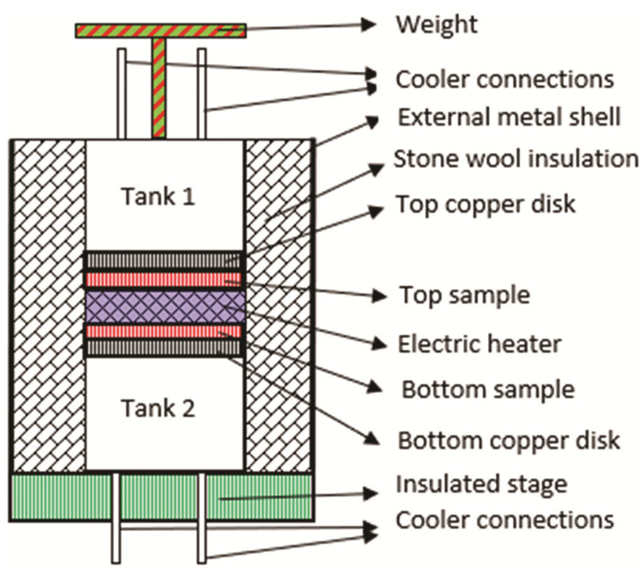

Fig. 4 — Schematic drawing of heat transfer coefficient test chamber

2.3 Test Methods

2.3.1 Thermal Conductivity Coefficient and Thermal Resistivity

Thermal conductivity [heat conduction coefficient (W/m°C) and thermal resistivity (m^2°C/W)] values of the samples were measured according to EN 12667 standard and evaluated based on the calculation methods/formulas outlined in ASTM C1045 standard. The experimental chamber is shown in Fig. 4. Two very similar samples are placed over and under the electric heater. All samples have the same diameters (113±0.1 mm) and thicknesses of around 5 mm (Table 1). For a specific experiment, top and bottom sample thicknesses are within 10 % range to each other. Two independent heat transfer coefficient and thermal resistance measurements were completed for each of the experiments.

2.3.2 Sound Absorption Coefficient

Sound absorption coefficient was measured by TestSens Sound Tube (BIAS) with twin-tube which can run according to ASTM E-2611, ASTM E-1050, ISO 10534-2 [53]. The inner diameters of the small tube and large tube are 29 mm and 100 mm respectively and the frequency range is 50 Hz-6400 Hz. Rigid materials such as glass fibre/epoxy disk was prepared with diameter of about 28 mm for small tube and 99 mm for large tube to overcome vibrational/noisy peak. Then the void between rigid sample and tube (1 mm) was filled by Vaseline gel. However, non-rigid materials such as nonwoven blankets were prepared keeping the tube diameters 29 mm and 100 mm.

2.3.3 Air Permeability Test

Air permeability of stone wool blanket and nonwoven blanket with PAN nanofibre and nonwoven blanket with silica aerogel was measured by Prowhite K008 Ait Test device under 100 Pa pressure using EN ISO 9237 standard. Air permeability of glass/epoxy composite was not measured.

3 Results and Discussion

As seen in Fig. 5, the air permeability decreases in the order of stone wool blanket, nonwoven blanket with silica aerogel, and then nonwoven blanket with PAN nanofibre. This result is also expected from the observation of these samples' compactness. The air permeability of stone wool is about 475 mm/s, while that of nonwoven fabric with aerogel is about 410 mm/s. It can be seen that the addition of PAN fibres significantly decreases the air permeability of nonwoven fabric in contrast to aerogels. This is because of the more compact structure of the PAN nanofibre web, wherein the pores between nanofibres are in the range of nanometre dimension or under micrometer dimension [Figs 1(a) and (b)]. Stone wool has the highest value when compared with nonwoven structures, because stone wool has more open structure than nonwoven structures.

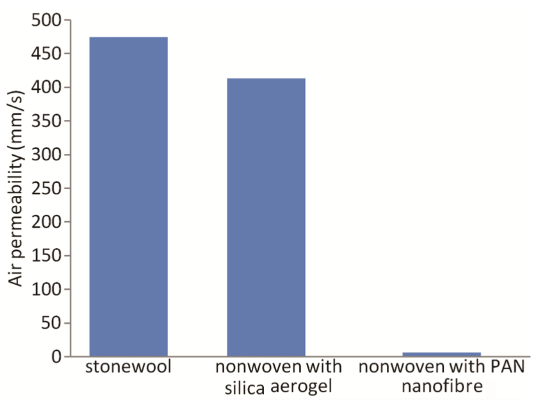

Fig. 5 — Air permeability test results

Table 2 — Heat transfer coefficients

Samples	K_{TOP}, W/M°C	K_{BOT}, W/M°C
GCSW	0.078	0.079
GCSA	0.087	0.087
GCPN	0.087	0.085

According to Table 2, in all experiments, the conductivities of both the top and bottom samples are within the range of 0.001 W/m°C, comparing to its pair (top and bottom). This fact is an essential indicator that the experiments are conducted quite precisely. Glass fibre/epoxy composite with stone wool (GCSW) has a lower heat transfer coefficient (~ 10-15%) as compared to that having nonwoven blanket with silica aerogel (GCSA) and with PAN nanofibre (GCPN). This can be explained by the insulation power of dead air in large voids of the stone wool blanket as indicated by the highest air permeability (Fig. 5), as compared to nonwoven with silica aerogel and nonwoven with PAN nanofibre web, although silica aerogel particle itself has the least heat transfer coefficient (~ 0.012 W/mK) [54]. Comparison of glass fibre/epoxy composite with a nonwoven and silica aerogel (GCSA) and nanofibre with PAN nanofibre (GCPN) is found very interesting. Both glass fibre/epoxy composite having a nonwoven blanket with silica aerogel (GCSA) and with PAN nanofibre (GCPN) are found similar to each other. The insulation properties of the PAN nanofibre web depend on the many micro or nanopores between the nanofibres [Figs 1(a) and (b)], as in the case of silica aerogel pores. These micro or nanopores between the nanofibres decrease air permeability because of the very small dimension of voids; many pores result in decrease in the heat transfer coefficient due to the insulation power of dead air in this small void.

According to Fig. 6, the sound absorption performances of both GCPN and GCSA are found higher than that of glass fibre/epoxy composite with stone wool (GCSW) due to pore/void dimensions and material type(polymeric /inorganic material). As already known, both PAN nanofibre web and silica aerogels can have nano and/or micro pores, while stone wool has larger voids which lead to higher air permeability (Fig. 5). Larger voids may lead to fewer sound absorptions. On the other hand, PAN nanofibre and nonwoven are polymeric materials, while stone wool and silica aerogel are inorganic materials. It is known that polymeric materials are more elastic than rigid inorganic materials, thus leading to more energy absorption and damping properties, which can result in more sound absorption. The sound absorption coefficient of glass fibre/epoxy composite with nonwoven blanket and PAN nanofibre (GCPN) is

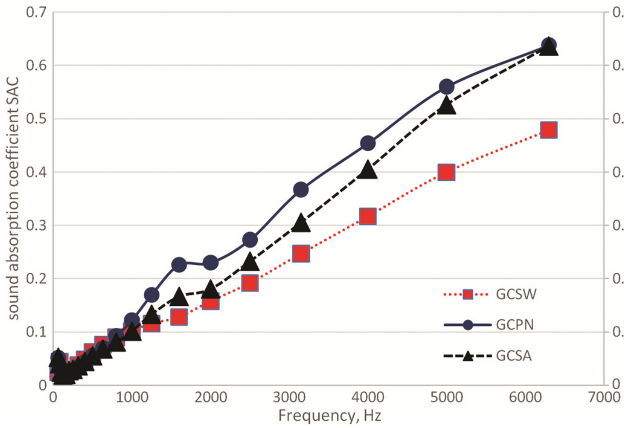

Fig. 6 — Absorption coefficients of all samples

slightly higher than that of glass fibre/epoxy composite with nonwoven blanket and silica aerogel (GCSA). This may be due to the elastomeric polymer structure of PAN nanofibre together with pores on the structure, which may lead to damper the sound vibration as compared to more rigid inorganic silica aerogel with pores.

4 Conclusion

The findings show that the thermal and sound insulation properties of several insulation layers used together with glass fibre fabric epoxy composite has wide application areas, such as in airplane, train, etc. It has been concluded that newly developed insulation layer for glass/epoxy composite, i.e. PAN nanofibre with PP nonwoven insulation layer, can be promising alternative insulation layers for glass fibre fabric epoxy composite and it also overcomes the brittle structure in conventional and commercially available stone wool insulation layer as well as insulation layer with silica aerogel, especially in vibrational working conditions

It has been observed that GCPN (glass fibre fabric epoxy composite with nanofibre) has highest sound absorption coefficient than others. The thermal insulation performance of GCPN may be acceptable when it is compared with GCSA (glass fibre fabric epoxy composite with silica aerogel) and GCSW (glass fibre fabric epoxy composite with stonewool); thermal insulation being~0.086 W/m°C and 0.087 W/m°C and 0.078 W/m°C respectively. However, it has some higher thermal conductivity coefficient as compared to GCSE.

Acknowledgement

Authors would like to thank TUBITAK (the Scientific and Technological Research Council of Turkey) for their financial support (#218M766) under the research project #218M766.

References

1 Vallittu PK, Lassila VP & Lappalainen RJDM, *Den Mat*, 10(2) (1994)116.
2 Selver E, Potluri P, Soutis C & Hogg P, *Compos Struct*, 122 (2015)57. doi: http://dx.doi.org/10.1016/ j.compstruct .2014.11.027.
3 Müller M, Liebsch A, Kupfer R, Stegelmann M & Gude M, *Procedia CIRP*, 85 (2019) 32. doi: https://doi.org/10.1016/ j.procir.2019.09.001.
4 Marzuki HFA & Jaafar M, *Procedia Chemist*, 19 (2016)871. doi: https://doi.org/10.1016/j.proche.2016.03.128.
5 Selver E, Potluri P, Hogg P & Soutis C, *Compos Part B*, 91 (2016)522. doi: http://dx.doi.org/10.1016/j.compositesb. 2015.12.035.
6 Sayyar M, Soroushian P, Sadiq MM, Balachandra A & Lu J, *Constr Build Mater*, 44 (2013)45. doi: https://doi.org/10. 1016/j.conbuildmat.2013.03.055.
7 Feih S, Mouritz AP, Mathys Z & Gibson AG, *J Compos Mat,* 41(19) (2007)2387. doi: 10.1177/0021998307075461.
8 Chinnasamy V, Pavayee Subramani S, Palaniappan SK, Mylsamy B & Aruchamy K, *J Mater Res Technol,* (2020). doi: https://doi.org/10.1016/j.jmrt.2020.01.061.
9 Rasana N, Jayanarayanan K, Deeraj BDS & Joseph K, *Compos Sci Technol*, 169 (2019)249. doi: https://doi.org/ 10.1016/j.compscitech.2018.11.027.
10 Yang Y, Li B, Chen Z, Xu T, Li Y, Fu R & Jing Y, *Text Res J*, 87(3) (2017)261. doi: 10.1177/0040517516629142.
11 Selver E, *Tekst ve Müh*, 26(113) (2019) 42.
12 Fu S-Y, Lauke B, Mäder E, Yue CY & Hu X, *Compos Part A*, 31(10) (2000)1117. doi:https://doi.org/10.1016/S1359-835X(00)00068-3.
13 Wu T, Huang Z-x, Wang D-z & Qu JP, *Adv Indust Eng Polym Res*, 2(3) (2019)93. doi: https://doi.org/10.1016 /j.aiepr.2019.06.003.
14 Kanie T, Fujii K, Arikawa H & Inoue K, *Den Mat*, 16(2) (2000)150.doi: 10.1016/s0109-5641(99)00097-4.
15 Wang S, Liu Y, Chen K, Xue P, Lin X & Jia M, *J Polym Res*, 27(4) (2020)1. doi: https://doi.org/10.1007/s10965-020-02063-y.
16 Kim J, Jeong M, Böhm H, Richter J & Modler N, *Compos Part B*, 181 (2020)107590. doi: https://doi.org/10.1016/j. compositesb.2019.107590.
17 Lee N-J & Jang J, *Compos Sci Technol,* 60(2) (2000)209. doi: https://doi.org/10.1016/S0266-3538(99)00122-0.
18 Tillotson TM & Hrubesh LW, *J Non-Cryst Solids,* 145 (1992)44. doi: https://doi.org/10.1016/S0022-3093(05) 80427-2.
19 Aegerter MA, Leventis N & Koebel MM, *Aerogels Handbook* (Springer New York), 2011. doi: https://doi.org/ 10.1007/978-1-4419-7589-8.
20 Dorcheh AS & Abbasi MH, *J Mater Process Technol,* 199(1) (2008)10. doi: https://doi.org/10.1016/j.jmatprotec.2007. 10.060.
21 Sehaqui H, Zhou Q & Berglund LA, *Compos Sci Technol,* 71(13) (2011)1593. doi: https://doi.org/10.1016 /j.comp scitech.2011.07.003.
22 Forest L, Gibiat V & Woignier T, *J Acoust Soc Am,* 105(2) (1999)1383. doi: https://doi.org/10.1121/1.426539.

23 Parmenter KE & Milstein F, *J Non-Cryst Solids*, 223(3) (1998)179. doi: https://doi.org/10.1016/S0022-3093(97)00430-4.

24 Durães L, Maia A & Portugal A, *J Supercritical Fluids*, 106 (2015)85. doi: https://doi.org/10.1016/j.supflu.2015.06.020.

25 Zhang Y-G, Zhu Y-J, Xiong Z-C, Wu J & Chen F, *ACS Appl Mater Interfaces*, 10(15) (2018)13019. doi: https://doi.org/10.1021/acsami.8b02081.

26 Geslain A, Groby JP, Romero-García V, Cervera F & Sanchez-Dehesa J, *J Non-Cryst Solids*, 499 (2018)283. doi: https://doi.org/10.1016/j.jnoncrysol.2018.07.021.

27 Li D, Zhang C, Li Q, Liu C, Arıcı M & Wu Y, *Appl Therm Eng*, 165 (2020)114547. doi: https://doi.org/10.1016/j.applthermaleng.2019.114547.

28 Liebner F, Pircher N & Rosenau T, *Bacterial NanoCellulose Aerogels in Bacterial Nanocellulose*, edited by M Gama , F Dourado and S Bielecki (Elsevier, Amsterdam), 2016, p. 73. doi: https://doi.org/10.1016/C2013-0-16061-8.

29 Gurav JL, Jung I-K, Park H-H, Kang ES & Nadargi DY, *J Nanomater*, (2010)1. doi: https://doi.org/10.1155/2010/409310.

30 Bhuiyan MAR, Wang L, Shaid A, Jahan I & Shanks RA, *J Mat Sci*, 55(6) (2020)2405. doi: 10.1007/s10853-019-04203-2.

31 Mazraeh-shahi ZT, Shoushtari AM & Bahramian AR, *Procedia Mat Sci*, 11 (2015)583. doi: https://doi.org/10.1016/j.mspro.2015.11.081.

32 Chakraborty S, Pisal A, Kothari V & Rao AV, *J Adv Mat Sci*, 2016 (2016)2495623. doi: https://doi.org/10.1155/2016/2495623.

33 Shafi S, Navik R, Ding X & Zhao Y, *J Non-Cryst Solids*, 503-504 (2019)78. doi: https://doi.org/10.1016/ j.jnoncrysol.2018.09.029.

34 Haq EU, Zaidi SFA, Zubair M, Karim MRA, Padmanabhan SK & Licciulli A, *Energy Buildings*, 151 (2017)494. doi: https://doi.org/10.1016/j.enbuild.2017.07.003.

35 Zhu Z, Yao H, Wang F, Dong J, Wu K, Cao J & Long D, *Macromol Mater Eng*, 304(5) (2019)1. doi: 10.1002/mame.201800676.

36 Li C, Cheng X, Li Z, Pan Y, Huang Y & Gong L, *J Non-Cryst Solids*, 457 (2017)52. doi: https://doi.org/10.1016/j.jnoncrysol.2016.11.017.

37 Zhou T, Cheng X, Pan Y, Li C, Gong L & Zhang H, *Appl Surf Sci*, 437 (2018)321. doi: https://doi.org/10.1016/j.apsusc.2017.12.146.

38 Yang T, Xiong X, Venkataraman M, Mishra R, Novak J & Militky J, *J Text Inst*, 110(2) (2019)196. doi: 10.1080/00405000.2018.1472540.

39 Talebi Z, Soltani P, Habibi N & Latifi F, *Const Build Mat*, 220 (2019)76. doi: https://doi.org/10.1016/ j.conbuildmat.2019.06.031.

40 Forest L, Gibiat V & Hooley A, *J Non-Cryst Solids*, 285(1) (2001)230. doi: https://doi.org/10.1016/S0022-3093(01)00458-6.

41 El-Hage Y, Hind S & Robitaille F, *J Text Fiber Mater*, 1 (2018)1. doi: https://doi.org/10.1177/2515221117751154.

42 Naito K, Yang J-M, Xu Y & Kagawa Y, *Carbon*, 48(6) (2010)1849. doi: https://doi.org/10.1016/j.carbon. 2010.01.031.

43 Xiang H-f, Tan S-x, Yu X-l, Long Y-h, Zhang X-l, Zhao N & Xu J, *Chinese J Polym Sci*, 29(6) (2011)650. doi: 10.1007/s10118-011-1079-x.

44 Ozturk MK, Nergis FB & Candan C, *Polym Advan Technol*, 29(4) (2018)1255. doi: 10.1002/pat.4236.

45 Liu H, Wang D, Zhao N, Ma J, Gong J, Yang S & Xu J, *Mater Res Innov*, 18(sup4) (2014)888. doi: 10.1179/1432891714Z.000000000797.

46 Rabbi A, Bahrambeygi H, Shoushtari AM & Nasouri K, *J Eng Fiber Fabric,* 8(4) (2013)36. doi: 10.1177/155892501300800412.

47 Sabetzadeh N, Bahrambeygi H, Rabbi A & Nasouri K, *J Micro Nano Let*, 7(7) (2012)662. doi: 10.1049/mnl.2012.0375

48 Karamanos A, Hadiarakou S & Papadopoulos AM, *Energy Buildings*, 40(8) (2008) 1402. doi: https://doi.org/10.1016/j.enbuild.2008.01.004.

49 Vrána T & Björk F, *Const Build Mat*, 23(5) (2009)1775. doi: https://doi.org/10.1016/j.conbuildmat.2008.10.014.

50 Nagy B, Simon TK & Nemes R, *J Therm Anal Calorim*, 139(1) (2020)169. doi: 10.1007/s10973-019-08384-5.

51 Andres B, Livkiss K, Hidalgo JP, Hees PV, Bisby L, Johansson N & Bhargava, *J Fire Sci*, 36(4) (2018)315. doi: 10.1177/0734904118783942.

52 Forouharmajd F & Mohammadi Z, *IJST-T Mech Eng*, 42(1) (2018)73. doi: 10.1007/s40997-017-0078-0.

53 Mühendislik B, TestSens Sound Tube. https://bias.com.tr/53/90/sensorler-ve-olcum-sistemleri/testsens-soundtube-empedans-tubu.php (accessed on 7 May 2020)

54 CABOT, Aerogel Particles. https://www.cabotcorp.com/solutions/ products-plus/aerogel/particles (accessed on 2 May 2020).